

Collective diffusion, self-diffusion and freezing criteria of colloidal suspensions

Adolfo J. Banchio^{a)} and Gerhard Nägele^{b)}

Fachbereich Physik, Universität Konstanz, Postfach 5560, D-78457 Konstanz, Germany

Johan Bergenholtz

Department of Physical Chemistry, Göteborg University, S-412 96 Göteborg, Sweden

(Received 16 February 2000; accepted 22 May 2000)

In this paper, we examine collective and self-diffusion properties of dispersions of spherically shaped colloidal particles at intermediate and long times. Our analysis is based on a fully self-consistent (rescaled) mode coupling theory (MCT) adjusted to describe the overdamped dynamics in concentrated suspensions of neutral and charged colloidal particles. The dynamical quantities studied in dependence on various experimentally controllable system parameters are the particle mean-squared displacement, long-time collective and self-diffusion coefficients, dynamic structure factors, nonexponentiality factors and collective and self-memory functions. The results of our theoretical treatment are compared with Brownian dynamics computer simulation data, experiment and other existing theories. It is shown that the rescaled MCT can be successfully applied to a wide range of dynamical properties. Our calculations reveal in particular an exponential long-time mode of the dynamic structure factor for a limited range of wave numbers and at sufficiently high concentrations. A dynamic scaling behavior of the dynamic structure factor and self-intermediate scattering function is predicted for the important case of salt-free charge-stabilized suspensions. As a consequence of the dynamic scaling, the static freezing criterion for colloids by Hansen and Verlet [Phys. Rev. **184**, 151 (1969)] is shown to be equivalent with the dynamic criterion by Löwen *et al.* [Phys. Rev. Lett. **70**, 1557 (1993)] related to long-time self-diffusion. © 2000 American Institute of Physics. [S0021-9606(00)50332-8]

I. INTRODUCTION

The dynamics of suspensions of spherical colloidal particles has been extensively studied in the past by means of various light scattering techniques.^{1–3} Part of the interest in these systems arises from the fact that these well-characterized dispersions can serve as model systems for more complex colloids relevant to the chemical and pharmaceutical industry. Furthermore, since the relevant length and time scales of colloids are easily accessible experimentally, colloidal model systems are good test beds for scrutinizing theoretical methods originally developed in atomic condensed matter physics and adjusted to describe the microstructure and diffusion of Brownian systems.

Unlike simple fluids, in which the molecular motion is ballistic and determined only by the molecular force law, the colloidal dynamics is dissipative due to the intervening solvent which gives rise to Brownian particle motion and many-body hydrodynamic interactions (HI). The presence of long-range HI and, quite frequently, also of polydispersity in particle sizes and interactions complicates the theoretical treatment of the colloidal dynamics considerably.

The static and short-time dynamic properties of bulk dispersions of monodisperse and polydisperse colloidal spheres

are well understood both from the experimental^{1,4–10} and theoretical^{7–9,11–15} point of view. On the other hand, the theoretical prediction of dynamic properties at intermediate and long times is far more difficult due to the occurrence of memory effects which depend both on direct and hydrodynamic interparticle forces. Exact analytical results for long-time diffusional properties are in fact known to date only for hard-sphere dispersions in the limit of small concentrations.^{16–20} For the more interesting case of concentrated dispersions, approximations have to be introduced to allow for further progress.

In a number of recent articles, we have used a (rescaled) mode coupling theory (MCT) for the calculation of long-time rheological and related diffusional properties of colloidal suspensions.^{21–24} For concentrated hard-sphere dispersions, we employed a short-time hydrodynamic rescaling procedure in the spirit of Medina-Noyola²⁵ and Brady,^{26,27} to approximate the strong influence of the HI on the particle dynamics. The findings from the rescaled MCT have been compared with experiments and Brownian dynamics (BD) computer simulations, and good agreement is observed.^{21,22} From our MCT calculations in Ref. 22, we were led to interesting predictions concerning the general validity of certain empirically found generalized Stokes–Einstein (GSE) relations linking low-shear viscoelastic properties to diffusion coefficients. Most of the GSE relations investigated in Ref. 22 were shown to hold reasonably well for hard-sphere dispersions, whereas the violation of the same GSE relations is

^{a)}Present Address: Division of Chemistry and Chemical Engineering, 210-41, California Institute of Technology, Pasadena, CA 91125, USA.

^{b)}Author to whom correspondence should be addressed. Electronic mail: Gerhard.Naegle@Uni-Konstanz.de

predicted in case of charge-stabilized suspensions.

In this paper, we extend the aforementioned analysis on the performance of the (rescaled) MCT by exploring now its predictions concerning collective and self-diffusion properties at intermediate and long times. Our results are exemplified for hard-sphere dispersions and de-ionized charge-stabilized dispersions in order to illustrate the different dynamic behavior of systems with short-range and long-range direct interactions. Although the MCT has been formulated recently also for colloidal mixtures with an arbitrary number of components,^{23,24,28} we restrict ourselves here to monodisperse and slightly polydisperse systems. We calculate and analyze various measurable dynamic properties including the dependence of the dynamic structure factor $S(q,t)$ on the wave number q and correlation time t , the particle mean squared displacement (MSD) $W(t)$, and the nonexponentiality factor $\Delta(q)$ which characterizes the overall nonexponential decay of $S(q,t)$. In calculating $\Delta(q)$, we also account for small size polydispersity effects which are of importance at small q . Furthermore, the density dependence of various long-time diffusion coefficients, and the density dependence and asymptotic time dependence of the irreducible memory functions related to collective and self diffusion are investigated.

To assess the accuracy of the MCT results, we compare with results obtained from experiments, BD simulations and some other existing theories. From this comparison the (rescaled) MCT will emerge as a useful approximate method for predicting diffusional properties, without requiring any adjustable parameter. By analyzing the analytical properties of the dynamic structure factor, we show that in MCT the hard-sphere $S(q,t)$ exhibits an exponentially decaying long-time form for volume fractions $\Phi > 0.2$ and for wave numbers near the value, q_m , where the maximum of the static structure factor $S(q)$ occurs. The exponential long-time mode can be characterized by a long-time collective diffusion coefficient $D_C^L(q_m)$, which decreases with increasing concentration. For de-ionized charge-stabilized suspensions, we predict a dynamic scaling behavior of $S(q,t)$ and of the self-intermediate scattering function, $G(q,t)$, in terms of a characteristic wave number and relaxation time related to the geometric mean particle distance. The MCT is consequently shown to map the static Hansen–Verlet freezing criterion²⁹ (cf. also Ref. 30) to the dynamic freezing criterion of Löwen *et al.*³¹

The paper is organized as follows: In Sec. II, we develop the general framework of the self-consistent (rescaled) MCT equations for $S(q,t)$ and for $G(q,t)$, and we outline its numerical implementation. In Sec. III we give the details of how collective and self-diffusional properties are determined in MCT. This section includes further a discussion of the asymptotic time dependence and scaling of $S(q,t)$, $G(q,t)$ and of the associated collective memory functions. Numerical results for diffusional properties of hard-sphere and charge-stabilized dispersions are presented and analyzed in Sec. IV, in comparison with computer simulations, experiment and some other existing theories on colloidal dynamics. Our final conclusions are contained in Sec. V.

II. MODE COUPLING THEORY OF COLLOIDAL DIFFUSION

We consider a monodisperse suspension of colloidal spheres of diameter $\sigma = 2a$ dispersed in a Newtonian solvent. The correlation of density fluctuations in the equilibrium state is described by the dynamic structure factor, defined as^{1,32}

$$S(q,t) = \left\langle \frac{1}{N} \sum_{l,p=1}^N e^{i\mathbf{q} \cdot (\mathbf{R}_l(t) - \mathbf{R}_p(0))} \right\rangle, \quad (1)$$

where \mathbf{q} is the scattering wave vector of modulus q , N is the number of colloidal particles in the scattering volume, $\mathbf{R}_l(t)$ is the position vector pointing to the center of sphere l , and $\langle \dots \rangle$ denotes an equilibrium ensemble average. The dynamic structure factor is the central statistical mechanical quantity describing the collective dynamics of colloidal particles. For times t much larger than the momentum relaxation time $\tau_B \approx 10^{-8}$ s, the colloidal dynamics is governed by the many-body Smoluchowski equation which describes the relaxation of the particle positions under the presence of direct and hydrodynamic forces.³ Within the time range where the Smoluchowski equation applies, HI can be considered to act instantaneously.

By using a projection operator formalism and an appropriate decomposition of the Smoluchowski equation, the following time evolution equation for $S(q,t)$ has been derived:^{23,33–36}

$$\begin{aligned} \frac{\partial}{\partial t} S(q,t) = & -q^2 D_C^S(q) S(q,t) \\ & - \int_0^t du M_C^{\text{irr}}(q,t-u) \frac{\partial}{\partial u} S(q,u), \end{aligned} \quad (2)$$

where $D_C^S(q) = D^0 H(q)/S(q)$ is a q -dependent short-time collective diffusion coefficient. Here, D^0 is the Stokes–Einstein diffusion coefficient of a colloidal sphere of radius a , and $H(q)$ is the hydrodynamic function. The latter quantity accounts for the configuration-averaged effect of the HI on the short-time dynamics.^{1,3} Without HI, $H(q) = 1$ independent of q , whereas undulations in $H(q)$ with a q -dependence similar to that of $S(q)$ are indicative of the influence of HI.^{7,8,10,37}

The first term on the right-hand-side of Eq. (2) determines the initial exponential decay of $S(q,t)$, which takes place within the short-time regime $\tau_B \ll t \ll \tau_a$, where $\tau_a = a^2/D^0 \approx 10^{-4} - 10^{-3}$ s is the time required for a non-interacting particle to diffuse a distance comparable to its own size. The integral term on the right-hand-side of Eq. (2) containing the irreducible collective memory function $M_C^{\text{irr}}(q,t)$ accounts for memory effects originating from collective particle motion. This memory term gives rise to an overall slower and, in general (cf. Sec. IV), nonexponential decay of $S(q,t)$ at intermediate times $t \approx \tau_a$ and at long times $t \gg \tau_a$.

An exact microscopic expression for $M_C^{\text{irr}}(q,t)$ was derived in Refs. 33, 35 and 38. This expression is used as the starting point for introducing a lowest order mode coupling approximation, following the work on simple and super-

cooled liquids,^{39,40} resulting in a self-consistent set of equations for calculating the dynamic structure factor of colloidal systems with their overdamped particle dynamics. While this scheme has been extended very recently to colloidal mixtures²³ and provides an opportunity for the inclusion of far-field HI, which is the prevailing part of the HI in dilute charge-stabilized colloids,^{23,28} the present results are obtained from the MCT applied to monodisperse fluid systems with HI disregarded. For the comparison with experimental data on concentrated hard-sphere dispersions, where the strong influence of many-body HI has to be accounted for, we describe this influence approximately by combining the MCT with a short-time hydrodynamic rescaling procedure as used already in Refs. 21 and 22 (cf. Sec. III). In Refs. 21 and 22, it was shown that that the hydrodynamically rescaled MCT of hard-sphere dispersions leads to good agreement with experimental findings on viscoelastic and diffusional properties.

In MCT, the collective memory function is approximated without HI by

$$M_C^{\text{irr}}(q,t) = \frac{D^0}{2n(2\pi)^3} \times \int d^3k [V_C(\mathbf{q},\mathbf{k})]^2 S(k,t) S(|\mathbf{q}-\mathbf{k}|,t), \quad (3)$$

with the vertex amplitude^{33,35,39,41,42}

$$V_C(\mathbf{q},\mathbf{k}) = \hat{\mathbf{q}} \cdot \mathbf{k} n c(k) + \hat{\mathbf{q}} \cdot (\mathbf{q}-\mathbf{k}) n c(|\mathbf{q}-\mathbf{k}|), \quad (4)$$

related to collective diffusion. Here, $c(q) = [1 - 1/S(q)]/n$ is the Fourier-transformed two-body direct correlation function, $\hat{\mathbf{q}} = \mathbf{q}/q$, and n denotes the number density of particles. The vertex amplitude $V_C(\mathbf{q},\mathbf{k})$ in Eq. (4) is derived in the so-called convolution approximation, where the contribution of static three-point direct correlations is neglected. The convolution approximation for the collective vertex amplitude is used in most of the recent applications of the MCT to atomic^{34,39,40} and colloidal dynamics.^{21,22,33,36,43,44} Its application gives rise to a consistent glass transition scenario in form of an ergodic–nonergodic transition of the particle dynamics.^{39,40,42,45} It should be mentioned that an approximation for $V_C(\mathbf{q},\mathbf{k})$ different from Eq. (4) has been suggested by Hess and Klein.⁴⁶ However, as pointed out already in Ref. 35, the Hess and Klein vertex approximation leads to poor results for collective dynamic properties in comparison with experimental and computer simulation data on charged and neutral colloidal particles.

The mode coupling scheme has been developed also for self-diffusional properties, related to the self-intermediate scattering function

$$G(q,t) = \langle e^{i\mathbf{q} \cdot (\mathbf{R}_1(t) - \mathbf{R}_1(0))} \rangle. \quad (5)$$

The time evolution of the scattering function $G(q,t)$ is described by the memory equation^{28,34,35}

$$\frac{\partial}{\partial t} G(q,t) = -q^2 D_S^S G(q,t) - \int_0^t du M_S^{\text{irr}}(q,t-u) \frac{\partial}{\partial u} G(q,u), \quad (6)$$

where the irreducible memory function, $M_S^{\text{irr}}(q,t)$, describing self-diffusion is approximated in MCT by

$$M_S^{\text{irr}}(q,t) = \frac{D^0}{(2\pi)^3 n} \times \int d^3k [V_S(\mathbf{q},\mathbf{k})]^2 S(k,t) G(|\mathbf{q}-\mathbf{k}|,t). \quad (7)$$

In Eq. (6), D_S^S is the short-time self-diffusion coefficient which is equal to the initial slope of the particle mean-squared displacement. For vanishing HI, D_S^S reduces to D^0 , and the vertex amplitude $V_S(\mathbf{q},\mathbf{k})$ is approximated by

$$V_S(\mathbf{q},\mathbf{k}) = \hat{\mathbf{q}} \cdot \mathbf{k} \left(1 - \frac{1}{S(k)} \right). \quad (8)$$

Notice that $V_C(\mathbf{q},\mathbf{k})$ according to Eq. (4) corresponds to $2V_S(\mathbf{q},\mathbf{k})$ in the limit of large q . This limiting behavior is to be expected physically since $S(q,t) \approx G(q,t)$ when $q \gg q_m$. Eqs. (2)–(4) constitute a self-consistent set of nonlinear equations determining $S(q,t)$ for given static structure factor $S(q)$. The latter can be calculated independently for given pair potential using, e.g., well-established integral equation schemes.⁴⁷ Once $S(q,t)$ has been determined, $G(q,t)$ follows from solving Eqs. (6)–(8). A well-known feature of the MCT equations presented here is that they predict an idealized glass transition scenario. This scenario is characterized by the appearance of nonergodicity in Brownian systems above a certain concentration threshold, where $S(q,t)$ and $G(q,t)$ do not relax to zero and where the suspension viscosity diverges,^{23,40} consistent with experimental measurements on hard sphere^{43,48} and charge-stabilized particle systems.⁴⁹

In the following, we briefly outline the numerical method used in solving the coupled Eqs. (2)–(8). After re-expressing the integrals in the memory function expressions in Eqs. (3) and (7) in bipolar coordinates, the coupled MCT equations are solved numerically in discretized form using an algorithm developed by Fuchs *et al.*⁵⁰ A uniform wave number grid with typically 500 grid points, $q = i\Delta q$, is employed with a grid spacing $\Delta q = q_m/40$. The resulting MCT integral-difference equations are integrated forward in time starting from the known short-time behavior of $S(q,t)$ and $G(q,t)$. In performing the time derivative, the logarithms of $S(q,t)$ and $G(q,t)$ are used instead of these quantities themselves to improve on the numerical accuracy. As discussed in more detail in the following section, the irreducible memory functions of hard-sphere dispersions show a $t^{-1/2}$ singularity for $t \rightarrow 0$ arising from the singular nature of the pair potential. Advantage is taken of the analytically known short-time forms of $M_S^{\text{irr}}(q,t)$ and of $M_C^{\text{irr}}(q,t)$ for the integration over the first time steps where $S(k,t)$ and $G(k,t)$ can be described by their short-time forms.

The MCT equations presented so far have been obtained without HI. For concentrated hard-sphere dispersions, strong many-body HI effects have to be accounted for to be able to compare with experimental results. The incorporation of many-body HI into long-time diffusion is a very difficult task and has been accomplished so far only approximately. We, therefore, use a hydrodynamic rescaling procedure of the MCT results for concentrated hard-sphere dispersions which allows for quantitative comparison with experimental data.^{21,22} This procedure derives from the assumption that diffusion properties with HI can be factorized in a hydrodynamic part, given by the corresponding short-time property with HI included, and a purely structural part. The latter is calculated using the MCT equations [Eqs. (2)–(8)].

For the case of self-diffusion, the rescaling procedure amounts to approximating the particle mean-squared displacement $W(t) = \langle [\mathbf{R}_1(t) - \mathbf{R}_1(0)]^2 \rangle / 6$ and the long-time self-diffusion coefficient D_S^L , with HI included, by

$$W(t) \approx \left(\frac{D_S^S}{D^0} \right) W(t)^{\text{MCT}}, \quad (9)$$

corresponding to

$$D_S^L \approx \left(\frac{D_S^S}{D^0} \right) D_S^{L,\text{MCT}}. \quad (10)$$

The factorization approximation for D_S^L in Eq. (10) has been proposed initially by Medina-Noyola²⁵ and developed in more detail by Brady.²⁶ For the short-time self-diffusion coefficient of hard spheres, we use a semiempirical result suggested by Lionberger and Russel⁵¹

$$\frac{D_S^S(\Phi)}{D^0} = (1 - 1.56\Phi)(1 - 0.27\Phi), \quad (11)$$

which conforms to the rigorous dilute limit $D_S^S/D^0 = 1 - 1.83\Phi$, and which gives $D_S^S = 0$ at random close packing $\Phi \approx 0.64$.

A similar rescaling can be performed for the long-time collective diffusion coefficient $D_C^L(q_m)$ of hard spheres, defined by^{21,22,52}

$$D_C^L(q_m) = - \frac{1}{q_m^2} \lim_{t \rightarrow \infty} \frac{\partial}{\partial t} \log S(q_m, t), \quad (12)$$

in the concentration regime where $S(q_m, t)$ exhibits an exponential long-time mode. A collective long-time mode of $S(q_m, t)$ has indeed been observed in dynamic light scattering experiments on colloidal hard-sphere dispersions.⁵² The rescaling relation for $D_C^L(q_m)$ is explicitly given by

$$D_C^L(q_m) \approx H(q_m) D_C^{L,\text{MCT}}, \quad (13)$$

where $H(q_m)$ is the value of the hydrodynamic function at the wave number q_m characterizing the extent of the nearest neighbor shell around a particle. As shown in Refs. 21 and 22, the concentration dependence of $H(q_m)$ for hard spheres is well represented by the linear form

$$H(q_m) = 1 - 1.35\Phi, \quad (14)$$

for volume fractions up to the freezing transition.

We notice that the rescaled expression for $D_C^L(q_m)$ in Eq. (13), with q_m replaced by q , reduces to that for D_S^L in Eq. (10) in the long wave number regime $q \gg q_m$. It is further observed that the exact short-time form of $W(t)$ is recovered from Eq. (9) in the short-time regime.

The hydrodynamic rescaling procedure for colloidal hard spheres is semiempirical and does not reproduce the known exact dilute limits of the long-time transport coefficients. On physical grounds, one can expect Eq. (9) to apply only at sufficiently high concentrations, where each particle is surrounded by a well-defined dynamic cage of neighboring particles. A particle diffusing out of its cage very likely will pass one of the cage particles very closely, since the hard-sphere radial distribution function attains its maximum at contact distance. Due to the strongly reduced relative hydrodynamic mobility of two colloidal spheres near contact, the tracer particle will diffuse very slowly in the immediate neighborhood of its cage neighbor for a considerable amount of time, as adequately described by short-time self-diffusion, before leaving the cage leading to structural relaxation. This intuitive picture of cage diffusion provides a rationale for Eq. (9). The factorization approximation in Eq. (9) should not hold for charge-stabilized dispersions according to this picture, since long-range double layer repulsion prevents particles from diffusing so close to each other that lubrication forces come into play. On the contrary, the far-field part of the HI prevailing in dilute charge-stabilized dispersions is expected to promote the diffusion of the tracer particle out of its momentary cage, leading thus to a hydrodynamic enhancement of long-time self-diffusion. This enhancement should be contrasted with hard sphere dispersions where, in qualitative accord with Eq. (9), near-field HI causes the particles to diffuse slower at long times. The hydrodynamic enhancement of long-time self-diffusion in de-ionized charge-stabilized dispersions was predicted in Ref. 35 on the basis of simplified MCT calculations and exact low-density results. It should occur in all colloidal systems with long-range repulsive pair forces. Hydrodynamic enhancement of self-diffusion has been observed meanwhile in experiments and computer simulations on charge-stabilized dispersions,⁵³ and on quasi-two-dimensional colloids confined near a liquid-gas interface^{54,55} or between two closely spaced plates.⁵⁶

Since a rescaling procedure for charge-stabilized systems is not known to date, we will neglect in our calculations the influence of HI on these systems. For charge-stabilized systems, we expect the diffusional properties to be only moderately affected by HI, as supported by exact low-density effective hard-sphere calculations and simplified MCT calculations of D_S^L .³⁵ Our findings for the diffusional properties of charge-stabilized systems will be mainly compared with BD simulations. In these simulations, the influence of HI is disregarded due to the considerable difficulties in incorporating HI into simulations. We point out that the calculation of diffusional properties in MCT with HI disregarded is important to assess the accuracy of the treatment of many-body direct interactions.

III. CALCULATION OF DIFFUSIONAL PROPERTIES

Having reviewed the basic MCT equations, we address now the calculation of various diffusional properties. Furthermore, we discuss the asymptotic time behavior of $S(q, t)$ and related irreducible memory functions. Dynamic scaling relations are proposed for salt-free charge-stabilized dispersions, which relate the Hansen–Verlet static freezing criterion to a dynamical one proposed by Löwen *et al.*

The mean-squared displacement (MSD) can be determined from $G(q, t)$ according to

$$W(t) = - \lim_{q \rightarrow 0} \frac{\log G(q, t)}{q^2}. \quad (15)$$

At short times, $W(t)$ increases linearly in time with a slope D_S^S , followed by a sub-linear increase at intermediate times due to the retarding influence of the cage of neighboring particles. At long times, $W(t)$ is again linear with slope equal to the long-time self-diffusion coefficient D_S^L . The coefficient D_S^L follows thus from:

$$D_S^L = \lim_{t \rightarrow \infty} \frac{W(t)}{t}. \quad (16)$$

Using Eq. (6), D_S^L can be calculated alternatively from

$$D_S^L = \frac{D_S^S}{1 + \tilde{M}_S^{\text{irr}}(q \rightarrow 0, s \rightarrow 0)}, \quad (17)$$

where $\tilde{M}_S^{\text{irr}}(q, s)$ is the Laplace transform of $M_S^{\text{irr}}(q, t)$.

A suitable measure of the overall nonexponential decay of $S(q, t)$ for correlated particles is the nonexponentiality factor, $\Delta(q)$, defined as^{35,46,57,58}

$$\Delta(q) = 1 - \frac{\tau_C^S(q)}{\bar{\tau}(q)}. \quad (18)$$

The relaxation time $\tau_C^S(q) = S(q)/(q^2 D^0 H(q))$ characterizes the short-time decay of $S(q, t)$, whereas

$$\bar{\tau}(q) = \int_0^\infty dt \phi_C(q, t) = \tilde{\phi}_C(q, s = 0), \quad (19)$$

is the mean relaxation time of the normalized dynamic structure factor $\phi_C(q, t) = S(q, t)/S(q)$, with Laplace transform $\tilde{\phi}_C(q, s)$. Using Eq. (2), $\Delta(q)$ can be expressed in terms of the zero-frequency limit of the Laplace-transformed irreducible memory function, $\tilde{M}_C^{\text{irr}}(q, s)$, as

$$\Delta(q) = \frac{\tilde{M}_C^{\text{irr}}(q, s = 0)}{1 + \tilde{M}_C^{\text{irr}}(q, s = 0)}, \quad (20)$$

from which it follows that $0 \leq \Delta(q) \leq 1$. For weakly correlated particles with small deviations of $\phi_C(q, t)$ from its short-time form $\exp[-t/\tau_C^S(q)]$, $\Delta(q)$ attains values close to zero, whereas values close to one indicate strong particle correlations with a slow decay of $S(q, t)$.

Whereas theory predicts for monodisperse systems with pairwise additive HI that $\Delta(q \rightarrow 0) = 0$, experimental data extrapolate to finite values of $\Delta(q \rightarrow 0)$. This apparent contradiction was resolved in Refs. 57 and 58, where it was shown

that even tiny amounts of size polydispersity can give rise to values of the measured $\Delta(q \ll q_m)$ significantly larger than zero. For dispersions with a narrow size distribution, the experimentally determined dynamic structure factor is well approximated by the decoupling approximation form³⁵

$$S_D(q, t) = X(q)G_I(q, t) + [1 - X(q)]S_I(q, t), \quad (21)$$

with the scattering coefficient $X(q) \approx 9s^2$ essentially independent of q for wave numbers $q\bar{\sigma} < 0.5$. The size distribution is determined by the mean particle diameter $\bar{\sigma}$ and the relative standard deviation $s \ll 1$. The quantities $S_I(q, t)$ and $G_I(q, t)$ are the dynamic structure factor and self-intermediate scattering function of the idealized monodisperse system of particles of diameter $\bar{\sigma}$. In Refs. 57 and 59 it was shown for weakly polydisperse systems of strongly correlated particles that the first term on the right-hand-side of Eq. (21), which originates from self-diffusion, dominates the temporal decay of $S_D(q, t)$ at small q , since $S_D(0) \ll 1$ and $S_D(q, t) \leq S_D(q)$. As a consequence nonzero values for the nonexponentiality factor $\Delta_D(q)$ related to $S_D(q, t)$ are obtained for $q \rightarrow 0$. By accounting for size polydispersity on the basis of the decoupling approximation and using a simplified (i.e., not fully self-consistent) MCT solution for $S_I(q, t)$ and $G_I(q, t)$, good agreement was found for small q with experimentally determined nonexponentiality factors.^{35,57} In Sec. IV, fully self-consistent MCT results for $\Delta(q)$ are presented, resulting in improved agreement with experimental and BD simulation data at intermediate values of q .

We proceed now with a general discussion of the asymptotic time dependence of $S(q, t)$. Consider first a hard-sphere dispersion with HI ignored. The singular hard core potential leads to a nonanalytical behavior of the irreducible memory functions $M_C^{\text{irr}}(q, t)$ and $M_S^{\text{irr}}(q, t)$ for $t \rightarrow 0$. Within the MCT, we can deduce the asymptotic short-time dependence of the irreducible memory functions by employing in the vertex amplitudes in Eqs. (4) and (8) the large- q asymptotic form

$$S(q) \approx 1 - 12\Phi g(2a^+) \frac{j_1(2qa)}{qa} + \mathcal{O}(q^{-3}), \quad (22)$$

of the hard-sphere static structure factor $S(q)$. Here, $j_1(x)$ is the first-order spherical Bessel function, and $g(2a^+) \geq 1$ is the contact value of the hard-sphere radial distribution function $g(r)$. From an asymptotic short-time analysis of Eq. (3), we obtain with Eq. (22) the following result for the short-time form of $M_C^{\text{irr}}(q, t)$ (cf. Ref. 60 for details)

$$\tau_a M_C^{\text{irr}}(q, t) \approx \sqrt{\pi}(qa)^2 A_C^{\text{MCT}}(q; \Phi) \tau^{-1/2}, \quad (23)$$

as $\tau \ll 1$, where we have introduced the wave number dependent dimensionless time $\tau = q^2 D^0 t$. The coefficient A_C^{MCT} is given by

$$A_C^{\text{MCT}}(q; \Phi) = \frac{\sqrt{2}\Phi g(2a^+)^2}{\pi q a d(2qa)}, \quad (24)$$

with the function

$$d(x) = \frac{1}{1 - j_0(x) + 2j_2(x)}, \quad (25)$$

where $j_n(x)$ denotes the spherical Bessel function of order n . The contact value of the hard-sphere radial distribution function is given to good accuracy by the Carnahan–Starling formula

$$g(2a^+) = \frac{1 - \Phi/2}{(1 - \Phi)^3}, \quad (26)$$

within the fluid regime. The short-time divergence of $M_C^{\text{irr}}(q, t)$ proportional to $\tau^{-1/2}$ leads to the following short-time asymptotic form of the dynamic structure factor:

$$S(q, t) \approx S(q) - \tau + \frac{4}{3} \sqrt{\pi} A_C^{\text{MCT}}(q; \Phi) \tau^{3/2} + \mathcal{O}(\tau^2), \quad (27)$$

as can be deduced from a short-time expansion of Eq. (2) with Eq. (23) as input.

The related short-time asymptotics of the self-diffusion properties are easily derived from Eqs. (23) and (27) by employing that $G(q, t) \approx S(q, t)$, $d(2qa) \approx 1$, and $S(q) \approx 1$ in the limit of large- q :

$$\tau_a M_S^{\text{irr}}(q, t) \approx \sqrt{\pi} (qa)^2 A_S^{\text{MCT}}(q; \Phi) \tau^{-1/2} \quad (28)$$

and

$$G(q, t) \approx 1 - \tau + \frac{4}{3} \sqrt{\pi} A_S^{\text{MCT}}(q; \Phi) \tau^{3/2} + \mathcal{O}(\tau^2), \quad (29)$$

valid for $\tau \ll 1$. The coefficient A_S^{MCT} is equal to the right-hand-side of Eq. (24), with $d(2qa)$ replaced by one. The irreducible memory functions remain finite for $t \rightarrow 0$ in case of charge-stabilized dispersions, since the physical hard core is masked by soft long-range repulsive interactions. There are thus no terms in the short-time forms of the scattering functions proportional to $\tau^{3/2}$.

We have taken advantage of the short-time forms (23) and (28) in our numerical solution of the MCT equations for colloidal hard spheres. The MCT results for the short-time asymptotics should be compared with the exact asymptotic results²⁰ for $S(q, t)$ and $G(q, t)$, and for the associated irreducible memory functions. The exact asymptotic forms for hard spheres differ from the MCT results (23)–(29) only in the somewhat different coefficients A_C and A_S , which are given in terms of the MCT coefficients as $A_{C,S} = 2 A_{C,S}^{\text{MCT}}/g(2a^+)$. While not reproducing accurately the coefficients of the exact short-time forms of hard spheres, the MCT is at least qualitatively correct in predicting the exact asymptotic t -dependence. This is quite a remarkable finding since the approximations made in the MCT are aimed at describing diffusion effects at long times. We mention in this context that the transverse shear stress correlation function, $\Delta \eta(t)$, of colloidal hard spheres also exhibits a $t^{-1/2}$ divergence for $t \rightarrow 0$, in accord with MCT results for $\Delta \eta(t)$,^{22,24} which differ from the exact short-time asymptotics⁵¹ again by a factor of $g(2a^+)/2$.

Whereas the short-time forms of $S(q, t)$ and $G(q, t)$ for colloidal hard spheres are determined only by two-body effects and are thus obtained analytically for all physically allowed densities, the large- t asymptotics of these quantities is known analytically only up to linear order in Φ . In Refs. 18 and 20 it is shown that both $S(q, t)$ and $G(q, t)$ exhibit an algebraic-exponential long-time tail proportional to

$\tau^{-3/2} \exp[-\pi/2]$ to first order in Φ . While the long-time tail is too small to be of experimental relevance, its mere existence illustrates that $S(q, t)$ and $G(q, t)$ are in general non-exponentially decaying functions at long times.

Using in Eqs. (3) and (7) the small- q form of $S(q)$ to linear order in Φ , the same asymptotic long-time tails for $S(q, t)$ and $G(q, t)$ are recovered in MCT as in the exact low-density calculations, again up to somewhat different prefactors.

To linear order in Φ , it follows further from Eqs. (2) and (6) that the $\tau^{-3/2} \exp[-\pi/2]$ tail of the dynamic scattering functions corresponds to the same long-time tail in the associated irreducible memory functions. This illustrates the general observation that memory functions do not decay substantially faster than their associated scattering functions.

If $M_C^{\text{irr}}(q, t)$ would decay sufficiently faster than $S(q, t)$, then the memory integral in Eq. (2) could be de-convoluted for $t \gg \tau_a$ as

$$\int_0^t du M_C^{\text{irr}}(q, t-u) \frac{\partial}{\partial u} S(q, u) \approx \tilde{M}_C^{\text{irr}}(q, 0) \frac{\partial}{\partial t} S(q, t). \quad (30)$$

This would imply that $S(q, t)$ decays exponentially at long times according to

$$\phi_C(q, t) = e^{-q^2 \tilde{D}_C^L(q) t}, \quad t \gg \tau_a, \quad (31)$$

with a collective diffusion coefficient, $\tilde{D}_C^L(q)$, determined by

$$\tilde{D}_C^L(q) = \tilde{D}_C(q, s=0) = \frac{D_C^S(q)}{1 + \tilde{M}_C^{\text{irr}}(q, 0)}. \quad (32)$$

We have introduced here a wave number and frequency dependent diffusion kernel, $\tilde{D}_C(q, s)$, related to the normalized dynamic structure factor by³²

$$\tilde{\phi}_C(q, s) = \frac{1}{s + q^2 \tilde{D}_C(q, s)}. \quad (33)$$

The coefficient $\tilde{D}_C^L(q)$ is closely related to $\Delta(q)$ and $\bar{\tau}(q)$, since

$$\tilde{D}_C^L(q) = D_C^S(q) [1 - \Delta(q)]. \quad (34)$$

As pointed out already in Refs. 18–20, $\tilde{D}_C^L(q)$ as defined by Eq. (32) is actually a measure for the mean relaxation and not for the long-time relaxation of $S(q, t)$. An exponential long-time mode of $S(q, t)$ is characterized by $\tilde{D}_C^L(q)$ only when de-convolution (30) applies. However, we re-emphasize that this de-convolution is in general not valid so that $\tilde{D}_C^L(q)$ has to be distinguished from the genuine long-time collective diffusion coefficient $D_C^L(q)$, defined in Eq. (12), in the regime of volume fractions and wave numbers where the latter quantity exists. Hard-sphere results for $\tilde{D}_C^L(q_m)$ and $D_C^L(q_m)$ are presented in Sec. IV.

From a long-time MCT analysis of $S(q_m, t)$ for colloidal hard spheres without HI, we find an exponential long-time mode for concentrations $\Phi > 0.22$ where caging effects are sufficiently strong. This collective mode describes the decay of density fluctuations linked to the average extension,

$2\pi/q_m$, of a nearest neighbor cage. The associated coefficient $D_C^L(q_m)$ can be determined by analyzing the analytic properties of the Laplace-transformed dynamic structure factor, $\tilde{\phi}_C(q, z)$, in terms of the reduced frequency variable $z = s\tau_C^S(q)$. In the q - and Φ - regime where the collective mode exists, $D_C^L(q)$ is determined by the value $z = z_0(q) = -D_C^L(q)/D_C^S(q)$, with $-1 \leq z_0(q) < 0$, corresponding to a pole in $\tilde{\phi}_C(q, z)$. According to Eqs. (32) and (33), $z_0(q)$ is numerically obtained from the intercept of $\tilde{M}_C^{\text{irr}}(q, z)$ with the monotonically increasing function $f(z) = -[1 + z^{-1}]$. Notice here that $\tilde{M}_C^{\text{irr}}(q, z)$ is positively valued and monotonically decaying for real values of z where the Laplace integral of $M_C^{\text{irr}}(q, t)$ exists. In contrast to $D_C^L(q)$, $\tilde{D}_C^L(q)$ is determined by the value $z = \tilde{z}_0(q) = -\tilde{D}_C^L(q)/D_C^S(q)$, where $f(z) = \tilde{M}_C^{\text{irr}}(q, z=0)$. This gives rise to the inequality $\tilde{D}_C^L(q) \geq D_C^L(q)$ due to the monotonic z -dependence of $\tilde{M}_C^{\text{irr}}(q, z)$ and $f(z)$. The coefficient $\tilde{D}_C^L(q)$ obviously exists for any value of Φ and q . Our numerical analysis further reveals, e.g., that the collective long-time mode ceases to exist, even for values $\Phi > 0.22$, for wave numbers close to the first minimum of $S(q)$ located to the right of q_m .

A long-time analysis of the hard-sphere $S(q, t)$ similar to ours has been performed by Cichocki and Felderhof,^{19,20} on the basis of the so-called contact Enskog approximation (CEA). According to the CEA, a collective long-time mode of $S(q_m, t)$ appears for $\Phi > 0.15$, in qualitative accord with the MCT finding.

An exponential long-time decay of $S(q, t)$ for concentrated charged colloidal dispersions at wave numbers near q_m was proposed further by Cohen, de Schepper, and co-workers.^{61,62} Neglecting possible HI contributions, these authors approximate $D_C^L(q)$ by the so-called cage-diffusion coefficient, $D_c(q)$, defined by

$$D_c(q) = \frac{D^0 d(2qa)}{g(2a^+) S(q)}. \quad (35)$$

The factor $d(2qa)/S(q)$ describes the structural relaxation of a particle in its nearest-nearest neighbor cage. The contact value $g(2a^+)$ in Eq. (35) is equal to the contact value of an equivalent effective hard-sphere system, with an effective particle radius a determined from a best fit for $q = q_m$ of the experimentally observed $S(q)$ with the $S(q)$ of the equivalent hard sphere system.⁶² Notice that the contact value of the actual $g(r)$ is essentially equal to zero. Contrary to the MCT and CEA long-time results, which are based on the many-body Smoluchowski equation describing the dynamics of colloidal suspensions, the estimate (35) for $D_C^L(q)$ was proposed in analogy with results from the theory of dense atomic liquids. Therefore, the approach of Cohen, de Schepper *et al.* does not permit predicting the Φ -range and q -range where a collective long-time mode of $S(q, t)$ exists.

In recent work, Verberg, de Schepper and Cohen^{44,63} use expression (35) for $D_c(q)$ as an approximation for the short-time collective diffusion coefficient $D_C^S(q)$ of colloidal hard spheres, proposed to be valid for $q \approx q_m$ and $\Phi > 0.4$. They argue that the factor $D^0/g(2a^+)$ in Eq. (35), with a denoting now the actual hard-sphere radius, is useful as a phenomeno-

logical approximation for the short-time self-diffusion coefficient D_S^S . According to their reasoning, the hydrodynamic function $H(q)$ is then approximated near q_m by $d(2qa)/g(2a^+)$. Using $\Phi = 0.5$, this results in $H(q_m) \approx 0.20$, whereas $H(q_m) \approx 0.33$ according to the semiempirical expression in Eq. (14), in agreement with simulation data.⁶⁴ Moreover, $d(2qa)/g(2a^+)$ with $g(2a^+)$ as given in Eq. (26), has a Φ -dependence different from the linear one in Eq. (14). The quantity $d(2qa)/g(2a^+)$ is thus seen to be a rather poor approximation for $H(q_m)$.

The mean collective diffusion coefficient $\tilde{D}_C^L(q)$ of concentrated hard-sphere dispersions is calculated by Verberg *et al.* using a simplified MCT scheme.⁴⁴ This scheme amounts to approximating $S(k, t)$ and $G(k, t)$ in the MCT integral of Eq. (3) for all times and all wave numbers by the approximate short-time forms $\phi_C(k, t) \approx \exp[-k^2 D_c t]$ and $G(k, t) \approx \exp[-k^2 (D^0/g(2a^+)) t]$. Moreover, the bare Stokes-Einstein diffusion coefficient D^0 in Eq. (3) is replaced in their scheme by $D_S^S \approx D^0/g(2a^+)$, approximating the influence of HI in a mean-fieldlike way similar to earlier suggestions of Medina-Noyola²⁵ and Brady.²⁶ The exponential approximation used for $S(k, t)$ is rather crude, since the dynamic structure factor is nonexponential at intermediate and long times for wave numbers k different from q_m . Using that $G(k, t) \approx \exp[-k^2 W(t)]$, with small non-Gaussian effects neglected,⁴⁸ $G(k, t)$ is further seen to be nonexponential at intermediate times due to the sub-linear behavior of $W(t)$ (cf. Fig. 7). Contrary to the scheme of Verberg *et al.*, no *a priori* assumptions are made in the self-consistent MCT for the time dependence of the dynamic correlation functions on the right-hand-side of Eqs. (3) and (7). The self-consistent MCT is straightforwardly applicable also to moderately concentrated hard-sphere dispersions with $\Phi < 0.4$, and to systems with long-range soft potentials where $g(2a^+) \approx 0$, without the necessity of introducing an approximate effective hard-sphere picture [cf. Eq. (35) ff] for the latter case. The lack of self-consistency in the scheme of Verberg *et al.* and in the CEA excludes the possibility of obtaining an ergodicity-nonergodicity transition where $\tilde{D}_S^L(q)$ vanishes. Hard-sphere results for $D_S^L(q_m)$ and $\tilde{D}_S^L(q_m)$ are discussed in Sec. IV.

In the remaining part of this section we address in MCT without HI the scaling behavior of $S(q, t)$ and $G(q, t)$ for fluid systems with strong and long-range particle repulsion. Such systems are characterized in terms of a single physically relevant length scale, given by the geometric mean particle distance $\bar{r} = n^{-1/3}$. Important examples are de-ionized, i.e., salt-free, suspensions of charge-stabilized particles,^{1,32} and quasi-two-dimensional dispersions of superparamagnetic particles exposed to a perpendicular magnetic field.^{54,55}

The radial distribution function, $g(r)$, of these systems reveals a well-developed principal peak located at a radial distance, r_m , which is nearly equal to \bar{r} .¹⁴ Since $r_m \approx \bar{r}$, $g(r)$ depends essentially only on the reduced distance $\tilde{r} = r/r_m$. Likewise, since $q_m \times r_m \approx 2\pi$, $S(q)$ is only a function of the dimensionless wave number $\tilde{q} = q/q_m$. This scaling implies that static structure factors of systems with equal peak

height, $S(q_m)$, should nearly superimpose on top of each other when plotted vs \tilde{q} (cf. Sec. IV).

It is crucial to realize that the MCT equations [Eqs. (2)–(4) and (6)–(8)] determining $S(q,t)$ and $G(q,t)$ depend on q and t only through the reduced wave number \tilde{q} and the reduced time $\tilde{t}=t/\tau_{q_m}$, with $\tau_{q_m}=(q_m^2 D^0)^{-1}$, when scaled with respect to r_m . We demonstrate this scaling for self-diffusion. The scaling for $S(q,t)$ can be shown in a similar way. Introducing the dimensionless quantities \tilde{q} , $\tilde{k}=k/q_m$, \tilde{t} , and $\tilde{u}=u/\tau_{q_m}$, Eqs. (6) and (7) are readily rewritten as

$$\frac{\partial}{\partial \tilde{t}} G(\tilde{q}, \tilde{t}) = -\tilde{q}^2 G(\tilde{q}, \tilde{t}) - \tau_{q_m} \int_0^{\tilde{t}} d\tilde{u} M_S^{\text{irr}}(\tilde{q}, \tilde{t} - \tilde{u}) \frac{\partial}{\partial \tilde{u}} G(\tilde{q}, \tilde{u}), \quad (36)$$

with

$$\tau_{q_m} M_S^{\text{irr}}(\tilde{q}, \tilde{t}) = \int d^3 \tilde{k} [V_S(\tilde{\mathbf{q}}, \tilde{\mathbf{k}})]^2 S(\tilde{k}, \tilde{t}) G(|\tilde{\mathbf{q}} - \tilde{\mathbf{k}}|, \tilde{t}), \quad (37)$$

where we have used that $q_m^3/n \approx (2\pi)^3$ for the systems under consideration.

According to the reduced MCT equations, systems with equal $S(q_m)$ exhibit the same shapes of $S(q,t)$ and $G(q,t)$ as functions of q/q_m and t/τ_{q_m} . Provided that r_m is the only relevant length, the scaling of the dynamic correlation functions predicted in MCT appears to be physically reasonable, although we are not able to provide a general proof. It would be of interest to examine the scaling predictions further using BD simulations.

An immediate consequence of the dynamic scaling proposed in the MCT is that systems with identical $S(q_m)$ also have the same long-time self-diffusion coefficient. This one-to-one correspondence between $S(q_m)$ and D_S^L implies that the Hansen–Verlet static freezing criterion²⁹ and the dynamic criterion of Löwen *et al.*³¹ are equivalent. According to the Hansen–Verlet criterion, a monodisperse colloidal suspension freezes when $S(q_m) \approx 2.85$, whereas the freezing transition is characterized by the dynamic criterion through a value of D_S^L/D^0 close to 0.1. The dynamic criterion was found empirically from experiments and BD simulations (without HI) of systems with Yukawa-type repulsive pair potentials including the one-component plasma and hard-sphere dispersions as opposite limiting cases. In Sec. IV it is shown that the MCT applied to de-ionized charge-stabilized suspensions gives results in good agreement with the freezing values of $S(q_m)$ and D_S^L stated in the two criteria, which speaks in favor of the self-consistent MCT description of the simple liquid and colloidal dynamics.

The equivalence of the static and dynamic freezing criteria within MCT is a consequence of the single system length scale, which permits rescaling of the governing dynamic equations. Approximate agreement between the static and dynamic freezing criteria can be expected also for systems in which the primary static structure factor peak is the dominant feature of the static correlations.³⁴ Since the MCT

is an approximate theory for the dynamics, this finding may not provide any fundamental connections between the static and dynamic viewpoints of the freezing process, although studies⁶⁵ and suggestions⁶⁶ on this topic have been made.

In our discussion of the dynamic scaling behavior for systems with long-range repulsion, we have disregarded the possible influence of HI. The inclusion of HI effects inevitably introduces the (hydrodynamic) diameter σ as a second relevant length scale, through the appearance of hydrodynamic mobility tensors in quantities like the hydrodynamic function $H(q)$ (cf. Refs. 3, 32, and 67). As discussed before, far-field HI cause only a modest increase in D_S^L above its value without HI, so that the dynamic criterion can still be expected to hold qualitatively. Our expectation is supported by the work of Löwen *et al.*, where BD computer simulation results for D_S^L without HI are compared with experimental data.³¹

IV. RESULTS AND DISCUSSION

Numerical results for self- and collective dynamical properties of charge-stabilized and hard-sphere suspensions are presented in this section, and are compared with experimental work, BD simulations and other existing theories on colloidal dynamics. We first investigate charge-stabilized dispersions; hard-sphere systems are analyzed subsequently.

The effective pair potential, $u(r)$, acting between two charged particles is modeled as the superposition of a masked hard-core part of diameter σ with the repulsive part of the well-known Derjaguin–Landau–Verwey–Overbeek (DLVO) potential. The latter reads explicitly

$$\frac{u(r)}{k_B T} = 2Ka \frac{e^{-\kappa(r-2a)}}{r}, \quad r > 2a. \quad (38)$$

Here, K is a dimensionless coupling parameter given by

$$K = \frac{L_B}{2a} \left(\frac{Z}{1 + \kappa a} \right)^2, \quad (39)$$

where $L_B = e^2/(\epsilon k_B T)$ is the Bjerrum length for a suspending fluid of dielectric constant ϵ , and Z is the effective charge number of a colloidal particle in units of the elementary charge e . The screening parameter κ is determined by $\kappa^2 = 4\pi L_B [n|Z| + 2n_s] = \kappa_c^2 + \kappa_s^2$ where n_s is the number density of added 1-1 electrolyte. The parameter κ consists of a contribution, κ_c , due to counter-ions, which are assumed to be monovalent, and a second contribution, κ_s , arising from added electrolyte. Equation (38) is a good approximation for the effective pair potential of strongly charged particles, where the effective charge Z accounts for nonlinear screening effects.^{68,69}

We employ the well-established rescaled mean spherical approximation (RMSA) for calculating the static structure factor of charge-stabilized dispersions described by the potential in Eq. (38). The system parameters used in our MCT calculations and summarized in Table I describe various charge-stabilized systems studied in experimental,^{52,70–72} computer simulation^{71,73–75} and theoretical work.^{20,44,74,76} The parameters in Table I for the charged system (CS) are typical, e.g., for salt-free aqueous dispersions of highly

TABLE I. System parameters of charge-stabilized systems used in the RMSA/MCT calculations. The parameters describe systems studied by Härtl *et al.* (Ref. 71) (H), Gaylor *et al.* (Ref. 73) and López-Esquivel *et al.* (Ref. 76) (G+L), and Müller (Ref. 77) (M-ST, M-WX, and M-YZ). The data set CS models a typical macroion system, analyzed at various concentrations. The effective charge number Z and coupling parameter K are chosen such that the RMSA $S(q_m)$ is equal to the experimental or computer simulated peak height.

Parameters	Systems					
	H	G+L	M-ST	M-WX	M-YZ	CS
σ [nm]	80	46	100	100	100	100
$\phi \times 10^3$	0.52	0.44	1.15	1.28	1.3	1×10^{-5} –90
Z	500	...	329	475	364	500
n_s [$\mu\text{mol/l}$]	0.1	...	6.9	3.6	0.0	0.0
L_B [nm]	0.71	...	0.71	0.71	0.71	0.714
$\kappa\sigma$	0.25	0.149	0.9	0.7	0.28	0.0009–2.78
K	1754	752	366	879	721	312–1782

charged polystyrene spheres with $r_m \approx n^{-1/3}$. The effective charge numbers Z in the table are determined for the aqueous suspensions studied by Härtl *et al.*⁷¹ from matching the peak height of the RMSA $S(q)$ to the experimentally determined one. Likewise, for the systems studied by Gaylor *et al.*,⁷³ the RMSA $S(q_m)$ is fitted to the corresponding BD data by adjusting the coupling parameter K as described by López-Esquivel *et al.*⁷⁶ In this way, an optimized static input $S(q)$ is obtained for the coupled MCT equations.

The q -dependence of $S(q,t)$ for system G+L is shown in Fig. 1 to illustrate the relaxation of density fluctuation correlations. Our MCT results for $S(q,t)$ are compared with BD data of Gaylor *et al.*,⁷³ and with results of López-Esquivel *et al.*⁷⁶ derived from a single exponential approximation (SEXP) of the collective memory function $M_C^{\text{itr}}(q,t)$. The MCT $S(q,t)$ is seen to be in excellent agreement with the BD results even at the largest correlation time $t = 1.6$ ms considered, whereas the SEXP predicts that the structural relaxation proceeds too rapidly. The self-consistent MCT is thus a better approximation for intermediate and long times than the SEXP.

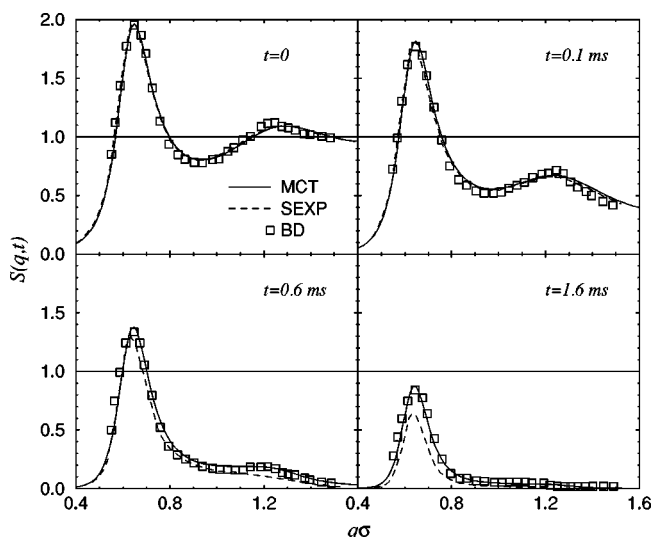


FIG. 1. Dynamic structure factor of charge-stabilized system G+L. Solid line: MCT results; dashed line: SEXP results from Ref. 76; open squares: BD data of Gaylor *et al.* (Ref. 73). System parameters as in Table I, with $D^0 = 9.5 \times 10^{-12} \text{ m}^2/\text{s}$.

We discuss next results for the time-dependence of $S(q,t)$, at fixed q , and for the nonexponentiality factor $\Delta_D(q)$ of charge-stabilized dispersions. In Fig. 2(a), the RMSA $S(q)$ for system H is shown together with the corresponding experimental and BD results by Härtl *et al.*⁷¹ While the RMSA $S(q)$ is matched only at q_m , there is good agreement with the BD data for all values of q . The experimental $S(q)$ is slightly larger than the RMSA and BD results at small q . This difference can be ascribed to a small amount of size polydispersity in the experimental sample with relative standard deviation $s \approx 0.06$. As indicated by the arrow, the principal peak of $S(q)$ is located at $q_m\sigma = 0.69 \approx q_2\sigma$.

Figure 2(b) displays MCT, BD, and experimental findings of $S(q,t)$ versus time for wave numbers q_1 and q_2 , the second one located at the peak of $S(q)$ and the first one at $q_1 \approx 0.87q_m$. The MCT predictions are in good qualitative agreement with the BD and experimental $S(q)$. The relaxation of density fluctuations of wavelength comparable with the extent of the nearest-neighbor cage, as described by $S(q_m,t)$, is seen to be considerably slower. Both curves reveal significant deviations from a single exponential form due to strong particle correlations.

The nonexponential decay of $S(q,t)$ is quantified by the nonexponentiality factors $\Delta_D(q)$ and $\Delta(q)$, introduced in Sec. III. Results for these quantities for system H and for the systems M-ST, M-WX, and M-YZ of Müller⁷⁷ are displayed in Figs. 3(a) and 3(b), respectively. Considering the statistical fluctuations in Fig. 3(a) in the experimental and BD data of $\Delta_D(q)$, calculated both without HI and using a size polydispersity of $s = 0.06$ according to the experimental estimate. Further shown in Fig. 3(a) is the MCT result for $\Delta(q)$ using $s = 0$, which illustrates the importance of size polydispersity effects at small q .

In Fig. 3(b), we compare MCT results for $\Delta_D(q)$, using $s = 0.05$, with the corresponding experimental data of Müller. Samples M-WX and M-ST are less correlated than sample M-YZ, due to the presence of residual electrolyte which screens the electrostatic interactions. The agreement with the experiment is good, regarding the fact that the MCT contains no adjustable parameter. For the most strongly correlated samples M-YZ and H, $\Delta_D(q)$ is somewhat overestimated in MCT. This can be at least partially attributed to

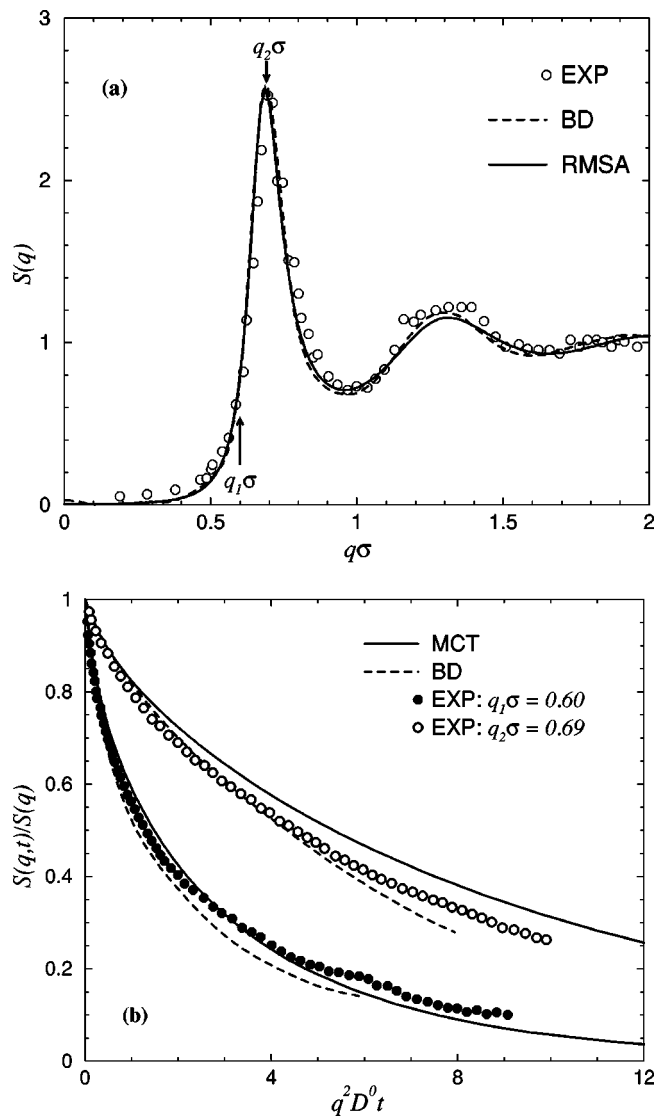


FIG. 2. $S(q)$ and normalized $S(q,t)$ for charge-stabilized system H (cf. Table I). (a) RMSA static structure factor in comparison with experimental and BD data of $S(q)$ taken from Härtl *et al.* (Ref. 71). The arrows locate the wave numbers $q_1\sigma=0.60$ and $q_2\sigma=0.69$. (b) $S(q,t)/S(q)$ at wave numbers q_1 and q_2 vs reduced time. Comparison between MCT results, and BD and experimental data from (Ref. 71).

far-field hydrodynamic effects, present in the experimental samples and neglected both in the MCT and BD calculations. As shown in Ref. 35 on the basis of a simplified and not fully self-consistent MCT scheme, far-field HI promotes the decay of density fluctuation correlations, leading thus to a modest decrease in $\Delta_D(q)$. The inclusion of far-field HI effects into a fully self-consistent MCT scheme is a very demanding numerical task (cf. Refs. 23 and 35) and is thus left to future work. It should be noted that the present MCT results for $\Delta_D(q)$ are in significantly better agreement with experiment and computer simulation data than the simplified MCT results published earlier in Ref. 35.

The scaling behavior of $S(q,t)$ and $G(q,t)$ for the deionized charge-stabilized systems CS and G+L with identical peak heights $S(q_m)$ is analyzed in Figs. 4(a) and 4(b). These systems are characterized by a single length scale \bar{r} . RMSA results for $S(q)$ versus reduced wave number q/q_m

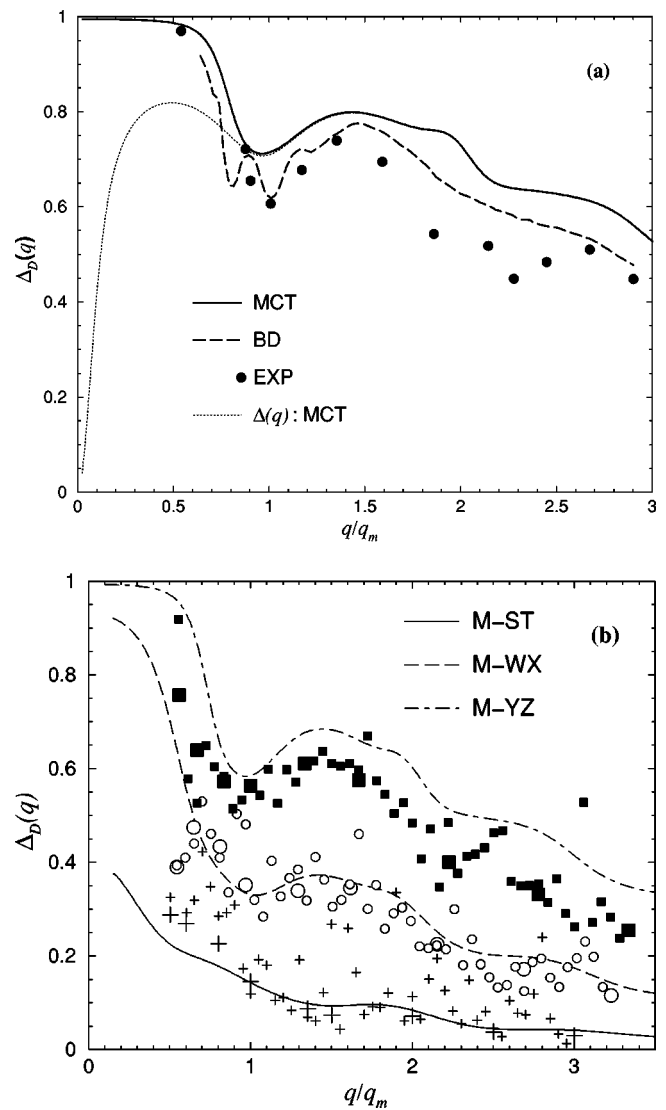


FIG. 3. Measurable nonexponentiality factor $\Delta_D(q)$ vs normalized wave number. (a) $\Delta_D(q)$ for system H with size polydispersity $s=0.06$. Solid line: MCT result; BD (dashed line) and experimental data (filled circles) are reproduced from Ref. 71. Dotted line: $\Delta(q)$ in MCT for $s=0$. (b) Comparison between MCT results (lines, as labeled) and experimental data of Müller (Ref. 77) for samples M-ST (+), M-WX (O), and M-YZ (filled \square) (cf. Table I), using $s=0.05$.

are depicted in Fig. 4(a). The static structure factors of samples CS and G+L are nearly identical when plotted versus \tilde{q} . The inset in the figure reveals differences at small q , which become visible only when $nc(q)$ is plotted versus \tilde{q} instead of $S(q)$. However, due to the smallness of $S(k \ll q_m)$ and due to the appearance of the factor k^4 in the integrals in Eqs. (3) and (7) defining the irreducible memory functions, these small- k differences are of no relevance in determining $S(q,t)$ and $G(q,t)$. This can be seen from Fig. 4(b), where MCT results for $\phi_C(q,t)$ are shown for three different wave numbers as a function of the reduced time t/τ_q . This figure clearly illustrates the scaling of $S(q,t)$ discussed in Sec. III, according to which systems with long-range particle repulsion and identical $S(q_m)$ possess equal dynamic structure factors as functions of the reduced parameters \tilde{q} and \tilde{t} .

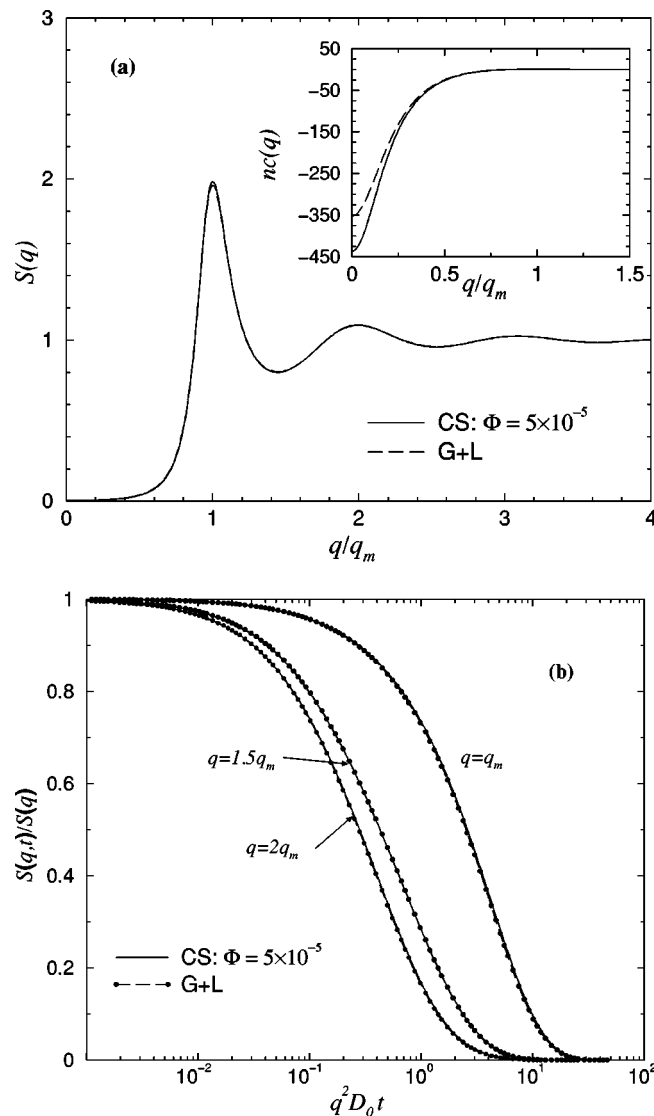


FIG. 4. MCT/RMSA results for $S(q)$ and $\phi_C(q,t)$ of system CS, with $\Phi = 5 \times 10^{-5}$, and system G+L (cf. Table I). (a) $S(q)$ and direct correlation function $nc(q)$ (inset) vs q/q_m as labeled in the figure. (b) Normalized $S(q,t)$ vs reduced time, for q -values as indicated.

The dependence of the MCT long-time self-diffusion coefficient D_S^L on the corresponding RMSA $S(q_m)$ is shown in Fig. 5 for the prototypical system CS. The coefficient D_S^L is a monotonically decaying function in $S(q_m)$ due to cage diffusion. For comparison, MCT results for D_S^L versus $S(q_m)$ of the remaining charge-stabilized systems listed in Table I are included additionally in the figure. Nearly all results lie on the master curve for system CS, in accordance with the scaling properties of $G(q,t)$. Only samples M-ST and M-WX, which contain residual electrolyte, are located slightly above the master curve.

According to the dotted lines shown in Fig. 5, the MCT master curve for de-ionized systems has a value of $D_S^L/D^0 = 0.1$ at $S(q_m) = 2.85$, in agreement with the freezing criteria of Hansen and Verlet and of Löwen *et al.* The scaling of $S(q,t)$ and D_S^L has been demonstrated in this work for charge-stabilized systems with DLVO-type pair potential. We reemphasize that the same scaling can be expected to

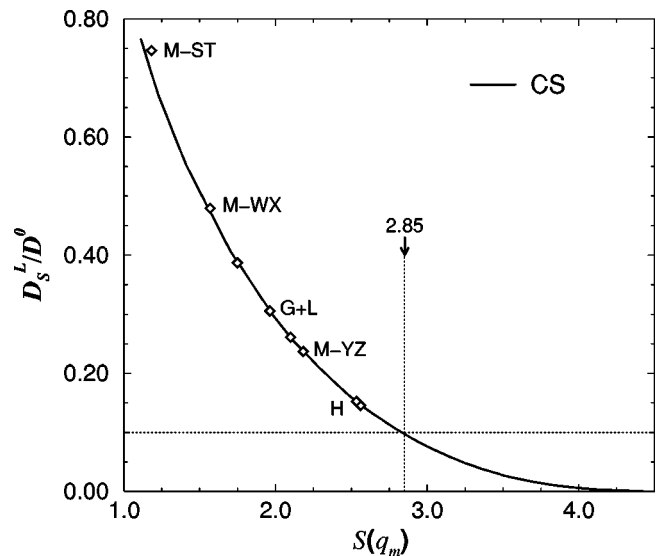


FIG. 5. Long-time self-diffusion coefficient D_S^L in MCT vs RMSA $S(q_m)$ for system CS (solid line), and remaining charge-stabilized systems listed in Table I (symbols). Dotted lines: freezing values $D_S^L/D^0 = 0.1$ and $S(q_m) = 2.85$, respectively.

hold, at least approximately, for all systems with long-range repulsive forces and masked excluded volume interactions.

In the following, we focus on the predictions of the MCT with regard to hard-sphere dispersions. The static input $S(q)$ is calculated using the Verlet–Weiss corrected Percus–Yevick approximation.⁴⁷ The MCT locates the (idealized) glass transition of hard-sphere dispersions at $\Phi = 0.525$,^{39,78} which is lower than the experimentally determined volume fraction.^{43,79} The caging of particles as described by the non-linear feedback terms in Eqs. (3) and (7) is thus overestimated in the MCT. While the MCT does not reproduce exactly the experimental glass transition concentration, it does reproduce the special dynamic features of the hard-sphere glass transition scenario.^{39,43,48,49} We follow, therefore, the work of Götze and co-workers in renormalizing the concentration dependence of the MCT-calculated dynamic hard-sphere properties according to $\Phi \rightarrow \Phi \times \Phi_g/0.525$. Here, Φ_g is not set equal to the experimental value of ~ 0.58 , but is estimated instead such that the MCT results for $D_S^L(\Phi)$ conform well at large concentrations with BD data obtained without HI in Ref. 75. This procedure gives $\Phi_g = 0.62$, with $D_S^L/D^0 = 0.1$ at the freezing transition concentration $\Phi_f = 0.49$, in accordance with the dynamic freezing criterion (cf. Fig. 6). The Φ -renormalization is used for all MCT results shown in Figs. 7–10. Whether or not a colloidal glass ultimately crystallizes and the rate at which it does so depends on the particle size distribution⁸⁰ and on gravitational effects.^{81,82} A study on suspensions of hard-spherelike particles found the glass to remain so indefinitely on earth but to crystallize under microgravity.⁸¹ Crystallization effects and gravitational influences are not incorporated into the idealized MCT, which is applied in this work to the fluid regime.

We remark that a value of $D_S^L/D^0 = 0.085$ rather close to 0.1 at freezing volume fraction Φ_f was obtained also by Fuchs⁸³ using MCT hard-sphere asymptotic laws, valid close to the glass transition concentration. The work of Fuchs cor-

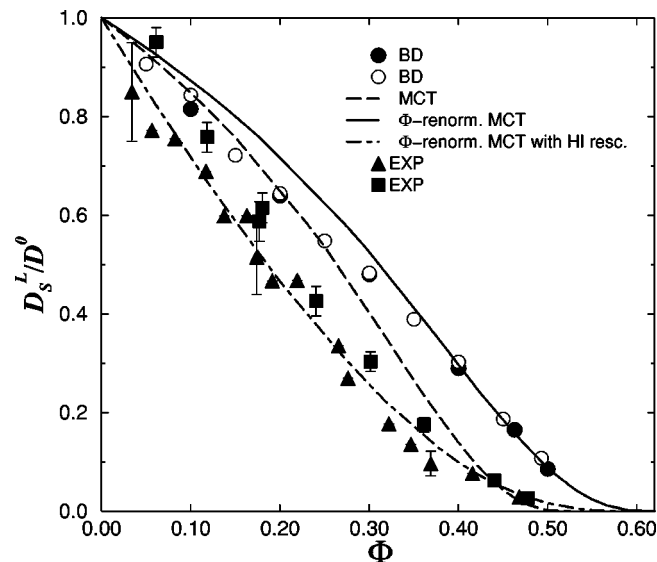


FIG. 6. Long-time self-diffusion coefficient for hard spheres as function of volume fraction. Filled circles: BD data of Cichocki and Hinsien (Ref. 75); open circles: BD data of Moriguchi (Ref. 89); dashed line: MCT results without Φ -renormalization and without HI-rescaling; solid line: Φ -renormalized MCT result; dashed-dotted line: Φ -renormalized and HI-rescaled MCT result; filled triangles: experimental data of van Megen and Underwood (Ref. 70); filled squares: experimental data of van Blaaderen *et al.* (Ref. 72).

rects earlier work of Indrani and Ramaswamy⁸⁴ who attempted to relate the freezing criteria of Hansen-Verlet to the one of Löwen *et al.* using simplified mode-coupling ideas.

For comparison with experimental hard-sphere results, we use the semiempirical hydrodynamic rescaling procedure described in Sec. III. According to Fig. 6, HI-rescaling using Eqs. (10) and (11) brings the MCT D_S^L into good agreement with the experimental data. The fact that experimental and HI-rescaled MCT values of D_S^L/D^0 at Φ_f are numerically

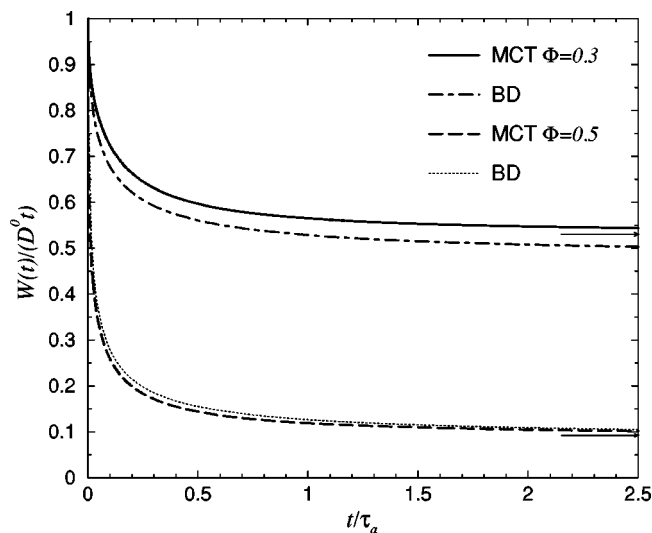


FIG. 7. Reduced MSD $W(t)/(D^0 t)$ for hard spheres at $\Phi=0.3$ (upper two curves) and $\Phi=0.5$ (lower two curves). Comparison between MCT results, and BD data taken from Ref. 75. The two horizontal line segments at the right ordinate indicate the values of the MCT reduced long-time self-diffusion coefficients.

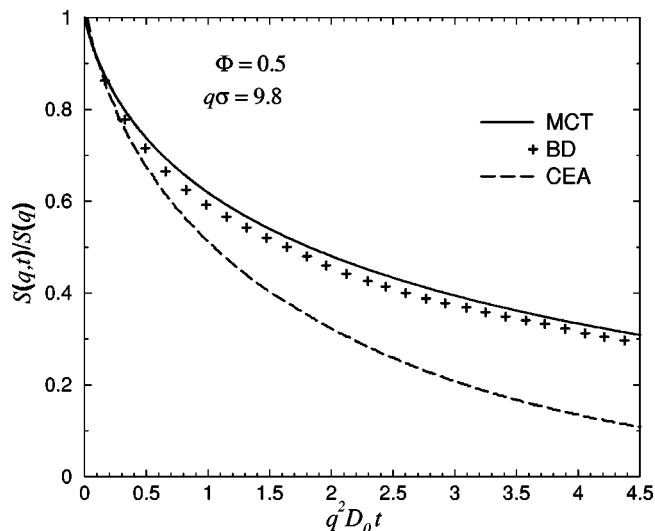


FIG. 8. Dynamic structure factor of hard spheres without HI for $\Phi=0.5$. Solid line: MCT result; dashed line: contact-Enskog approximation (CEA) result of Cichocki and Felderhof (Ref. 20); crosses: BD data from Ref. 20.

similar and consistently lower than 0.05 suggests the number 0.1 to be universal with HI included, i.e., to be independent of the pair potential, only when D_S^L is normalized by the short-time self-diffusion coefficient D_S^S instead of D^0 . For de-ionized charge-stabilized systems with $\Phi \leq 0.05$, D_S^S is well parameterized by the nonlinear form $D_S^S/D^0 = 1 - 2.5\Phi^{4/3}$ so that the short-time self-diffusion coefficient is insignificantly smaller than D^0 .^{13,32,85}

Hard-sphere MCT results for the reduced MSD $W(t)/(D^0 t)$ without HI are shown in Fig. 7 for two values of Φ , together with the corresponding BD results of Cichocki and Hinsien.⁷⁵ As seen, the agreement between MCT and BD improves with increasing concentration, with nearly coincident results even at intermediate times for $\Phi=0.5$.

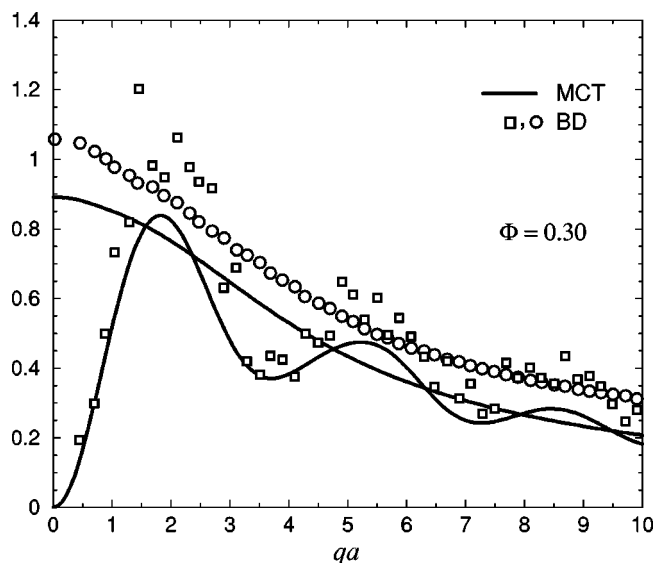


FIG. 9. Time-integrated irreducible memory functions $\tilde{M}_c^{\text{irr}}(q,0)$ and $\tilde{M}_s^{\text{irr}}(q,0)$ of hard spheres. Solid lines: MCT results. Symbols: BD data for $\tilde{M}_c^{\text{irr}}(q,0)$ (open squares) and $\tilde{M}_s^{\text{irr}}(q,0)$ (open circles) of Cichocki and Hinsien (Ref. 74).

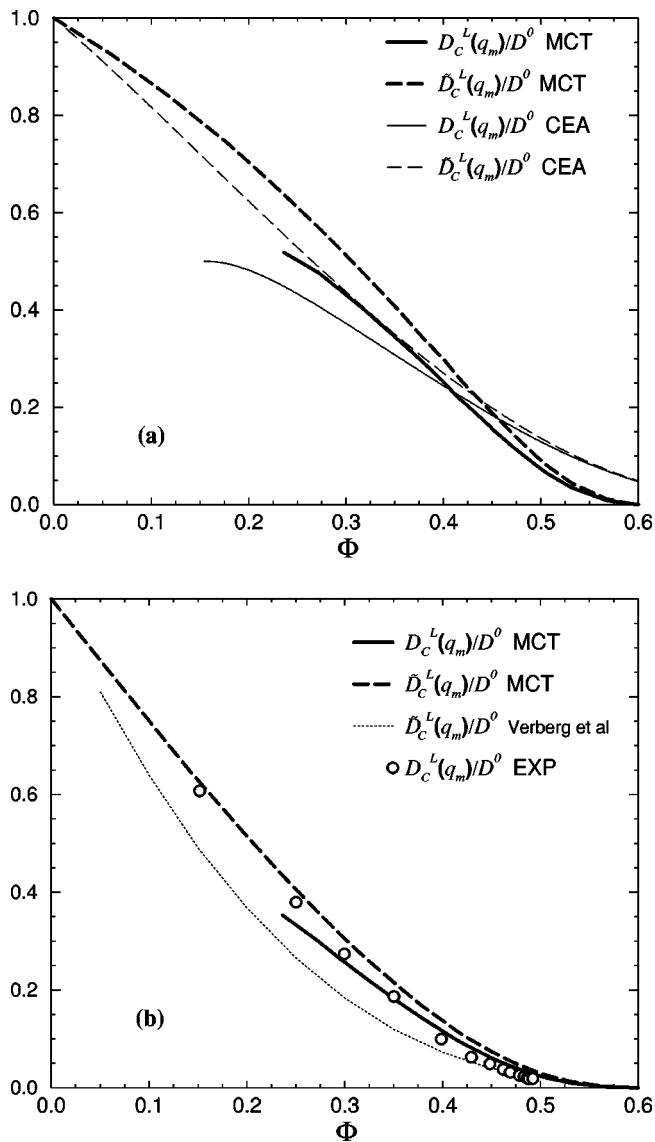


FIG. 10. (a) Hard-sphere normalized long-time and mean collective diffusion coefficients $D_C^L(q_m)$ and $\bar{D}_C^L(q_m)$, respectively, as functions of Φ . Comparison between MCT and CEA results without HI. Notice that $S(q_m, t)$ ceases to be an exponentially decaying function at long times for lower volume fractions. (b) Normalized $D_C^L(q_m)$ and $\bar{D}_C^L(q_m)$ vs Φ with HI. Open circles: exp. data for $D_C^L(q_m)/D^0$ from Segrè *et al.* (Ref. 52). Bold solid line: $D_C^L(q_m)/D^0$ in HI-rescaled MCT. Bold dashed line: $\bar{D}_C^L(q_m)/D^0$ in HI-rescaled MCT. Dotted line: $\bar{D}_S^L(q_m)/D^0$ according to Verberg *et al.* (Ref. 44).

Figure 8 includes MCT results for $\phi_C(q, t)$ without HI, at $q\sigma=9.8$ and $\Phi=0.5$, in comparison with BD and CEA results taken from Ref. 20. The BD and MCT results compare very well, whereas the relaxation of $S(q, t)$ is strongly overestimated in CEA. As pointed out already by its originators,²⁰ the CEA is designed for semidilute to moderately concentrated hard-sphere dispersions, where it is in good agreement with BD results. Its accuracy decreases with increasing concentration when mode coupling effects become strong.

BD data for the time-integrated irreducible memory functions have been reported in Ref. 74 and are included in Fig. 9 (for $\Phi=0.3$) together with the MCT predictions. The

function $\tilde{M}_C^{\text{irr}}(q, 0)$ can be expressed in terms of the non-exponentiality factor $\Delta(q)$ as $\tilde{M}_C^{\text{irr}}(q, 0) = \Delta(q)/(1 - \Delta(q))$, implying for monodisperse systems that $\tilde{M}_C^{\text{irr}}(q, 0) \propto q^2$ and $\Delta(q) \propto q^2$ for $qa \ll 1$. Contrary to $\tilde{M}_C^{\text{irr}}(q, 0)$, $\tilde{M}_S^{\text{irr}}(q, 0)$ is a monotonically decaying function. The overall q -dependencies are well reproduced by the MCT memory functions, with their values being consistently lower than the BD data. We expect the accuracy of the MCT predictions for $\tilde{M}_C^{\text{irr}}(q, 0)$ and $\tilde{M}_S^{\text{irr}}(q, 0)$ to improve for larger Φ , in accord with an analogous observation in Fig. 7 for $W(t)$. To our knowledge, however, there are so far no hard-sphere BD data for $\tilde{M}_{C,S}^{\text{irr}}(q, 0)$ available at higher volume fractions to compare with. Inclusion of HI increases the hard-sphere irreducible memory functions above its curves shown in Fig. 7, since near-field HI lead to an additional slowing down of particle diffusion.

In Fig. 10(a), we compare MCT and CEA results for the hard-sphere long-time collective diffusion coefficient $D_C^L(q_m)$, and for the mean collective diffusion coefficient $\bar{D}_C^L(q_m)$, obtained without HI. The CEA findings have been obtained by us following the CEA solution scheme described in Refs. 19 and 20. According to both theories, $D_C^L(q_m)$ ceases to exist below the concentration thresholds $\Phi_{\text{MCT}} = 0.22$ and $\Phi_{\text{CEA}} = 0.15$, respectively. While the CEA prediction for $D_C^L(q_m)$ is expected to be more accurate at lower Φ (being exact to first order in Φ), the MCT is a better approximation for $\Phi \geq 0.4$, where both diffusion coefficients are overestimated in the CEA. In accord with physical expectation, the long-time collective diffusion coefficient is seen in both theories to be smaller than the mean collective diffusion coefficient $\bar{D}_C^L(q_m)$, since the latter is related to the mean relaxation of $S(q_m, t)$.

HI-rescaled MCT results for $D_C^L(q_m)$ and $\bar{D}_C^L(q_m)$, obtained from multiplying the MCT coefficients by $H(q_m)$ [cf. Eqs. (13) and (14)] are compared in Fig. 10(b) with experimental data for $D_C^L(q_m)$ of Segrè *et al.*⁵² There is good qualitative agreement between theory and experiment in the range of Φ -values where, according to the MCT, $D_C^L(q_m)$ exists. Figure 10(b) displays also results for $\bar{D}_S^L(q_m)$ calculated by us using the nonself-consistent MCT scheme proposed by Verberg *et al.*⁴⁴ (cf Sec. III). Notice that the HI-rescaled MCT $\bar{D}_C^L(q_m)$ is substantially larger than the coefficient calculated using the scheme of Verberg *et al.*⁴⁴

Since the short-time self- and collective diffusion coefficients $D_C^S(q_m) = D^0 H(q_m)/S(q_m)$ and D_S^S of hard spheres according to Eqs. (14) and (11), respectively, are used as input in the hydrodynamic rescaling scheme, it is worthwhile to examine their concentration dependence in comparison with experimental results, and with approximations for these quantities proposed by Verberg and co-workers. The peak height $S(q_m)$ of the hard-sphere $S(q)$ is calculated using the Verlet–Weiss correction of the Percus–Yevick approximation. As seen from the inset in Fig. 11, $S(q_m)$ is contrary to $H(q_m)$ a distinctively nonlinear function of Φ , parametrized for $0 < \Phi < 0.55$ within 1% of accuracy by the form $S(q_m) \approx 1 + C\Phi g(2a^+)$, with $C = 0.664$ and $g(2a^+)$ according to Eq. (26).

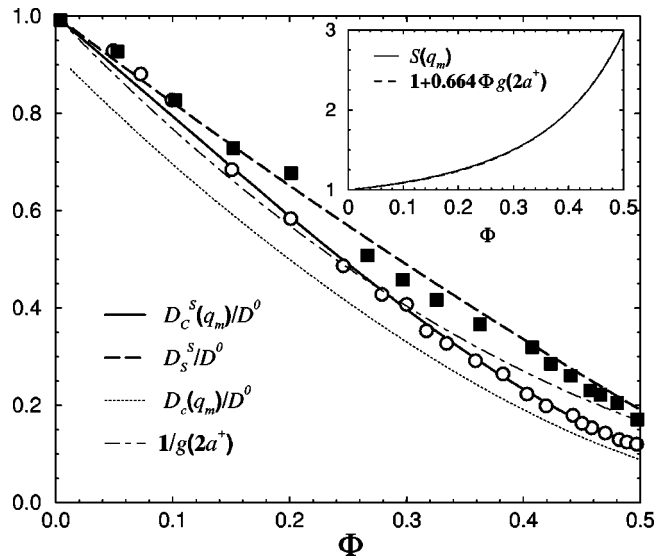


FIG. 11. Normalized short-time diffusion coefficients with HI. Bold solid line: $D_C^S(q_m)/D^0 = H(q_m)/S(q_m)$ with $H(q_m)$ according to Eq. (14); bold dashed line: D_S^S/D^0 according to Eq. (11). Open circles: experimental $D_C^S(q_m)/D^0$ from Ref. 8; filled squares: experimental D_0/D_S^S reproduced from Ref. 8. Dotted line: cage-diffusion coefficient $D_C(q_m)/D^0$ defined in Eq. (35). Dashed line: approximation for D_S^S according to Eq. (26). Inset: peak height of hard-sphere $S(q)$ according to Verlet–Weiss corrected Percus–Yevick approximation (solid line) and corresponding Φ -parametrization (dashed line).

The result for $D_C^S(q_m) = D^0 H(q_m)/S(q_m)$ in Fig. 11 is in excellent agreement with the experimental data of Segre *et al.*,⁸ which reflects the accuracy of Eq. (14) for $H(q_m)$. It is further seen that D_S^S according to Eq. (11) is in good agreement with the experimental data from 8. The approximations $D_C^S(q_m) \approx D_C(q_m)$ and $D_S^S \approx D^0/g(2a^+)$ suggested by Verberg and co-workers according to Eqs. (35) and (26), respectively, compare less favorable with the experimental findings, even in the limited concentration regime of $\Phi \geq 0.4$ where these empirical approximations have been proposed to apply.

V. CONCLUSIONS

In this paper we have presented and analyzed theoretical predictions for collective and self-diffusional properties of monodisperse and slightly polydisperse colloidal dispersions. Our results have been obtained from the self-consistent numerical solution of the (rescaled) MCT based on the many-particle Smoluchowski equation and applied to suspensions of charged and neutral colloidal spheres.

The dynamic structure factor and the mean-squared displacement of charge-stabilized systems calculated in MCT compare well with BD simulations and experimental results. The nonexponentiality factor of charged suspensions, with small polydispersity effects included, is remarkably well predicted by the theory, as demonstrated in comparison with experimental and BD results of $\Delta(q)$. For de-ionized suspensions of strongly repelling charged particles with well-developed nearest-neighbor shells, a dynamic scaling behavior of $S(q,t)$ and $G(q,t)$ is predicted in the fluid regime. From this scaling behavior, the equivalence of two seem-

ingly unrelated criteria for the onset of freezing is deduced. The proposed dynamic scaling of the dynamic scattering functions is based on the MCT, with HI disregarded, and on the scaling of the static structure factor with respect to the peak position q_m . We have confirmed the scaling of $S(q/q_m)$ as predicted in the RMSA using the accurate Rogers–Young integral equation scheme.^{32,86} It would be of interest to examine the dynamic scaling predictions further with the help of dynamic computer simulations.

For hard spheres, our MCT analysis reveals an exponential long-time mode of $S(q_m,t)$ for volume fractions $\Phi \geq 0.22$ well below the (idealized) glass transition concentration. This collective mode is associated with the long-time collective diffusion coefficient $D_C^L(q_m)$, which is smaller than the collective diffusion coefficient $\tilde{D}_C^L(q_m)$ related to the mean decay of $S(q_m,t)$. A long-time exponential decay of $S(q_m,t)$ has been predicted also for charge-stabilized dispersions of strongly correlated particles.²²

Our MCT results for colloidal hard spheres with renormalized volume fraction are in good qualitative accord with BD data for $S(q,t)$, $W(t)$, and for the time-integrated irreducible memory functions. The comparison with the BD data is even in quantitative agreement for the largest volume fraction $\Phi = 0.5$ considered. The asymptotic short-time and long-time forms of the hard sphere $S(q,t)$ and $G(q,t)$ are correctly predicted by the MCT, with amplitudes which are, however, not equal to the exact ones. It is possible to extend the good performance of the MCT for concentrated systems to hard-sphere dispersions at intermediate and small concentrations by combining the MCT with an Enskog-type generalized kinetic theory approach as proposed by Cichocki and Hinsen.⁷⁴ We are currently analyzing the predictions of this hybrid method.

A first-principles inclusion of (many-body) HI effects is to date a daunting task for any theory of concentrated dispersions. For colloidal hard spheres we have employed thus a semiempirical hydrodynamic rescaling of the MCT results, which allows for quantitative comparison with experimentally determined diffusional and viscoelastic properties. Physical arguments based on the cage picture have been provided to explain why the rescaling scheme is not applicable to systems with long-range repulsive pair forces. An approximate incorporation of leading order far-field HI in the MCT equations of monodisperse systems was provided by Nägele and Baur³⁵ and subsequently generalized to colloidal mixtures.^{23,28} This approach aims at describing the dynamics of charge-stabilized suspensions in the fluid regime. It differs from alternative attempts by Fuchs and Mayr³⁶ and by Verberg *et al.*⁴⁴ of incorporating many-body HI for colloidal hard spheres, in that the q -dependence of the MCT vertex functions is affected. That far-field HI should affect the structural relaxation of $S(q,t)$ and $G(q,t)$ in the liquid regime not only through the short-time coefficients $D_C^S(q)$ [cf. Eq. (2) ff] and D_S^S but also through a modified k -dependence of the vertex functions $V_C(\mathbf{q}, \mathbf{k})$ and $V_S(\mathbf{q}, \mathbf{k})$ is indicated by the weak coupling form of the self memory function in the limit of small potential and hydrodynamic forces.⁸⁷ However, the question whether HI influences not only the collo-

dal dynamics within the fluid regime but also the glass transition scenario remains unresolved.

The multicomponent version of the MCT with far-field HI included has been used for successfully predicting electro-hydrodynamic effects on the self-diffusion of a colloidal particle arising from the collective motion of small ions constituting its electric double layer.⁸⁸

In conclusion, our analysis has shown that the (rescaled) MCT is applicable not only close to the glass transition, but also to fluid colloidal systems with significant particle correlations. The self-consistent MCT provides at least qualitatively correct predictions of diffusional and viscoelastic properties of colloidal dispersions with a variety of interaction potentials.

ACKNOWLEDGMENTS

A.J.B. acknowledges financial support by the DAAD (Deutscher Akademischer Austauschdienst). We further acknowledge useful discussions with M. Fuchs (Technical University of Munich), J.F. Brady (California Institute of Technology), J.K.G. Dhont (Forschungszentrum Jülich), R. Klein (University of Konstanz), and financial support by the Deutsche Forschungsgemeinschaft (SFB 513).

- ¹P. N. Pusey, in *Liquids, Freezing and Glass Transition*, edited by J.-P. Hansen, D. Levesque, and J. Zinn-Justin (North-Holland, Amsterdam, 1991), pp. 763–942.
- ²W. B. Russel, D. A. Saville, and W. R. Schowalter, *Colloidal Dispersions* (Cambridge University Press, Cambridge, 1989).
- ³J. K. G. Dhont, *An Introduction to Dynamics of Colloids* (Elsevier, Amsterdam, 1996).
- ⁴W. Härtl and H. Versmold, *J. Chem. Phys.* **80**, 1387 (1984).
- ⁵R. Krause *et al.*, *J. Phys. C* **3**, 4459 (1991).
- ⁶N. J. Wagner *et al.*, *J. Chem. Phys.* **95**, 494 (1991).
- ⁷G. Nägele, O. Kellerbauer, R. Krause, and R. Klein, *Phys. Rev. E* **47**, 2562 (1993).
- ⁸P. N. Segrè, O. P. Behrend, and P. N. Pusey, *Phys. Rev. E* **52**, 5070 (1995).
- ⁹J. K. Phalakovkul *et al.*, *Phys. Rev. E* **54**, 661 (1996).
- ¹⁰W. Härtl, C. Beck, and R. Hempelmann, *J. Chem. Phys.* **110**, 7070 (1999).
- ¹¹V. Degiorgio, R. Piazza, and R. Jones, *Phys. Rev. E* **52**, 2707 (1995).
- ¹²G. Nägele, B. Mandl-Steininger, and R. Klein, *Prog. Colloid Polym. Sci.* **117**, 117 (1995).
- ¹³M. Watzlawek and G. Nägele, *Phys. Rev. E* **56**, 1258 (1997).
- ¹⁴M. Watzlawek and G. Nägele, *J. Colloid Interface Sci.* **124**, 170 (1999).
- ¹⁵A. J. Banchio, G. Nägele, and A. Ferrante, *J. Colloid Interface Sci.* **208**, 487 (1999).
- ¹⁶B. J. Ackerson and L. Fleishmann, *J. Chem. Phys.* **76**, 2675 (1982).
- ¹⁷S. Hanna, W. Hess, and R. Klein, *Physica A* **111**, 181 (1982).
- ¹⁸J. M. Rallison and E. J. Hinch, *J. Fluid Mech.* **167**, 131 (1986).
- ¹⁹B. Cichocki and B. U. Felderhof, *J. Chem. Phys.* **98**, 8186 (1993).
- ²⁰B. Cichocki and B. U. Felderhof, *Physica A* **204**, 152 (1994).
- ²¹A. J. Banchio, J. Bergenholtz, and G. Nägele, *Phys. Rev. Lett.* **82**, 1792 (1999).
- ²²A. J. Banchio, G. Nägele, and J. Bergenholtz, *J. Chem. Phys.* **111**, 8721 (1999).
- ²³G. Nägele, J. Bergenholtz, and J. K. G. Dhont, *J. Chem. Phys.* **110**, 7037 (1999).
- ²⁴G. Nägele and J. Bergenholtz, *J. Chem. Phys.* **108**, 9893 (1998).
- ²⁵M. Medina-Noyola, *Phys. Rev. Lett.* **60**, 2705 (1988).
- ²⁶J. F. Brady, *J. Chem. Phys.* **99**, 567 (1993).
- ²⁷J. F. Brady, *J. Fluid Mech.* **272**, 109 (1994).
- ²⁸G. Nägele and J. K. G. Dhont, *J. Chem. Phys.* **108**, 9566 (1998).
- ²⁹J. P. Hansen and L. Verlet, *Phys. Rev.* **184**, 151 (1969).
- ³⁰M. O. Robbins, K. Kremer, and G. S. Grest, *J. Chem. Phys.* **88**, 3286 (1988).
- ³¹H. Löwen, T. Palberg, and R. Simon, *Phys. Rev. Lett.* **70**, 1557 (1993).
- ³²G. Nägele, *Phys. Rep.* **272**, 215 (1996).
- ³³G. Szamel and H. Löwen, *Phys. Rev. A* **44**, 8215 (1991).
- ³⁴M. Fuchs, *Transp. Theory Stat. Phys.* **24**, 855 (1995).
- ³⁵G. Nägele and P. Baur, *Physica A* **245**, 297 (1997).
- ³⁶M. Fuchs and M. R. Mayr, *Phys. Rev. E* **60**, 5742 (1999).
- ³⁷A. P. Philipse and A. Vrij, *J. Chem. Phys.* **88**, 6459 (1988).
- ³⁸B. Cichocki and W. Hess, *Physica A* **141**, 475 (1987).
- ³⁹W. Götze, in *Liquids, Freezing and Glass Transition*, edited by J.-P. Hansen, D. Levesque, and J. Zinn-Justin (North-Holland, Amsterdam, 1991).
- ⁴⁰W. Götze and L. Sjögren, *Rep. Prog. Phys.* **55**, 241 (1992).
- ⁴¹L. Sjögren, *Phys. Rev. A* **22**, 2883 (1980).
- ⁴²U. Bengtzelius, W. Götze, and A. Sjölander, *J. Phys. C* **17**, 5915 (1984).
- ⁴³W. van Meegen and S. M. Underwood, *Phys. Rev. E* **49**, 4206 (1994).
- ⁴⁴R. Verberg, I. M. de Schepper, and E. G. D. Cohen, *Europhys. Lett.* **48**, 397 (1999).
- ⁴⁵E. Leutheusser, *Phys. Rev. A* **29**, 2765 (1984).
- ⁴⁶W. Hess and R. Klein, *Adv. Phys.* **32**, 173 (1983).
- ⁴⁷J.-P. Hansen and I. R. McDonald, *Theory of Simple Liquids*, 2 ed. (Academic, New York, 1986).
- ⁴⁸W. van Meegen, T. C. Mortensen, S. R. Williams, and J. Müller, *Phys. Rev. E* **58**, 6073 (1998).
- ⁴⁹C. Beck, W. Härtl, and R. Hempelmann, *J. Chem. Phys.* **111**, 8209 (1999).
- ⁵⁰M. Fuchs, W. Götze, I. Hofacker, and A. Latz, *J. Phys. (France)* **3**, 5047 (1991).
- ⁵¹R. A. Lionberger and W. B. Russel, *J. Rheol.* **38**, 1885 (1994).
- ⁵²P. N. Segrè, S. P. Meeker, P. N. Pusey, and W. C. K. Poon, *Phys. Rev. Lett.* **75**, 958 (1995).
- ⁵³W. Härtl *et al.*, *J. Phys.: Condens. Matter* **12**, A287 (2000).
- ⁵⁴K. Zahn, J. M. Méndez-Alcaraz, and G. Maret, *Phys. Rev. Lett.* **79**, 175 (1997).
- ⁵⁵B. Rinn, K. Zahn, P. Maass, and G. Maret, *Europhys. Lett.* **46**, 537 (1999).
- ⁵⁶R. Pesché and G. Nägele (unpublished).
- ⁵⁷P. Baur, G. Nägele, and R. Klein, *Phys. Rev. E* **53**, 6224 (1996).
- ⁵⁸G. Nägele and P. Baur, *Europhys. Lett.* **38**, 557 (1997).
- ⁵⁹G. Nägele, P. Baur, and R. Klein, *Physica A* **231**, 49 (1996).
- ⁶⁰A. J. Banchio, Ph.D. thesis, Universität Konstanz, Konstanz, Germany, 1999.
- ⁶¹I. M. de Schepper, E. G. D. Cohen, P. N. Pusey, and H. N. W. Lekkerkerker, *J. Phys. C* **1**, 6503 (1989).
- ⁶²P. N. Pusey, H. N. W. Lekkerkerker, E. G. D. Cohen, and I. M. de Schepper, *Physica A* **164**, 12 (1990).
- ⁶³R. Verberg, I. M. de Schepper, and E. G. D. Cohen, *Phys. Rev. E* **55**, 3143 (1997).
- ⁶⁴P. N. Segrè, O. P. Behrend, and P. N. Pusey, *Phys. Rev. E* **52**, 5070 (1995).
- ⁶⁵T. R. Kirkpatrick and P. G. Wolynes, *Phys. Rev. A* **35**, 3072 (1987).
- ⁶⁶J. Bergenholtz and M. Fuchs, *Phys. Rev. E* **59**, 5706 (1999).
- ⁶⁷S. Kim and S. J. Karrila, *Microhydrodynamics: Principles and Selected Applications* (Butterworth-Heinemann: Series in Chemical Engineering, Boston, 1991).
- ⁶⁸S. Alexander *et al.*, *J. Chem. Phys.* **80**, 5776 (1984).
- ⁶⁹H. Löwen, P. A. Madden, and J.-P. Hansen, *J. Chem. Phys.* **98**, 3275 (1993).
- ⁷⁰W. van Meegen and S. M. Underwood, *J. Chem. Phys.* **91**, 552 (1989).
- ⁷¹W. Härtl, H. Versmold, U. Witting, and P. Linse, *J. Chem. Phys.* **97**, 7797 (1992).
- ⁷²A. van Blaaderen, J. Peetermans, G. Maret, and J. K. G. Dhont, *J. Chem. Phys.* **96**, 4591 (1992).
- ⁷³K. J. Gaylor, I. K. Snook, W. van Meegen, and R. O. Watts, *J. Phys. A* **13**, 2513 (1980).
- ⁷⁴B. Cichocki and K. Hinsen, *Ber. Bunsenges. Phys. Chem.* **94**, 243 (1990).
- ⁷⁵B. Cichocki and K. Hinsen, *Physica A* **187**, 133 (1992).
- ⁷⁶J. A. López-Esquivel and J. L. Arauz-Lara, *J. Chem. Phys.* **96**, 1651 (1992).
- ⁷⁷J. Müller, Ph.D. thesis, Universität Kiel, Kiel, Germany, 1993.
- ⁷⁸J. L. Barrat, W. Götze, and A. Latz, *J. Phys.: Condens. Matter* **1**, 7163 (1989).
- ⁷⁹W. van Meegen, *Transp. Theory Stat. Phys.* **24**, 1017 (1995).
- ⁸⁰S. I. Henderson, T. C. Mortensen, S. M. Underwood, and W. van Meegen, *Physica A* **233**, 102 (1996).
- ⁸¹W. B. Russel *et al.*, *Langmuir* **13**, 3871 (1997).

⁸²J. Zhu *et al.*, *Nature (London)* **387**, 883 (1997).

⁸³M. Fuchs, *Phys. Rev. Lett.* **74**, 1490 (1995).

⁸⁴A. V. Indrani and S. Ramaswamy, *Phys. Rev. Lett.* **73**, 360 (1994).

⁸⁵E. Overbeck, C. Sinn, and M. Watzlawek, *Phys. Rev. E* **60**, 1936 (1999).

⁸⁶F. J. Rogers and D. A. Young, *Phys. Rev. A* **30**, 999 (1984).

⁸⁷J. A. Marqusee and J. M. Deutch, *J. Chem. Phys.* **73**, 5396 (1980).

⁸⁸M. Kollmann and G. Nägele (unpublished).

⁸⁹I. Moriguchi, *J. Chem. Phys.* **106**, 8624 (1997).